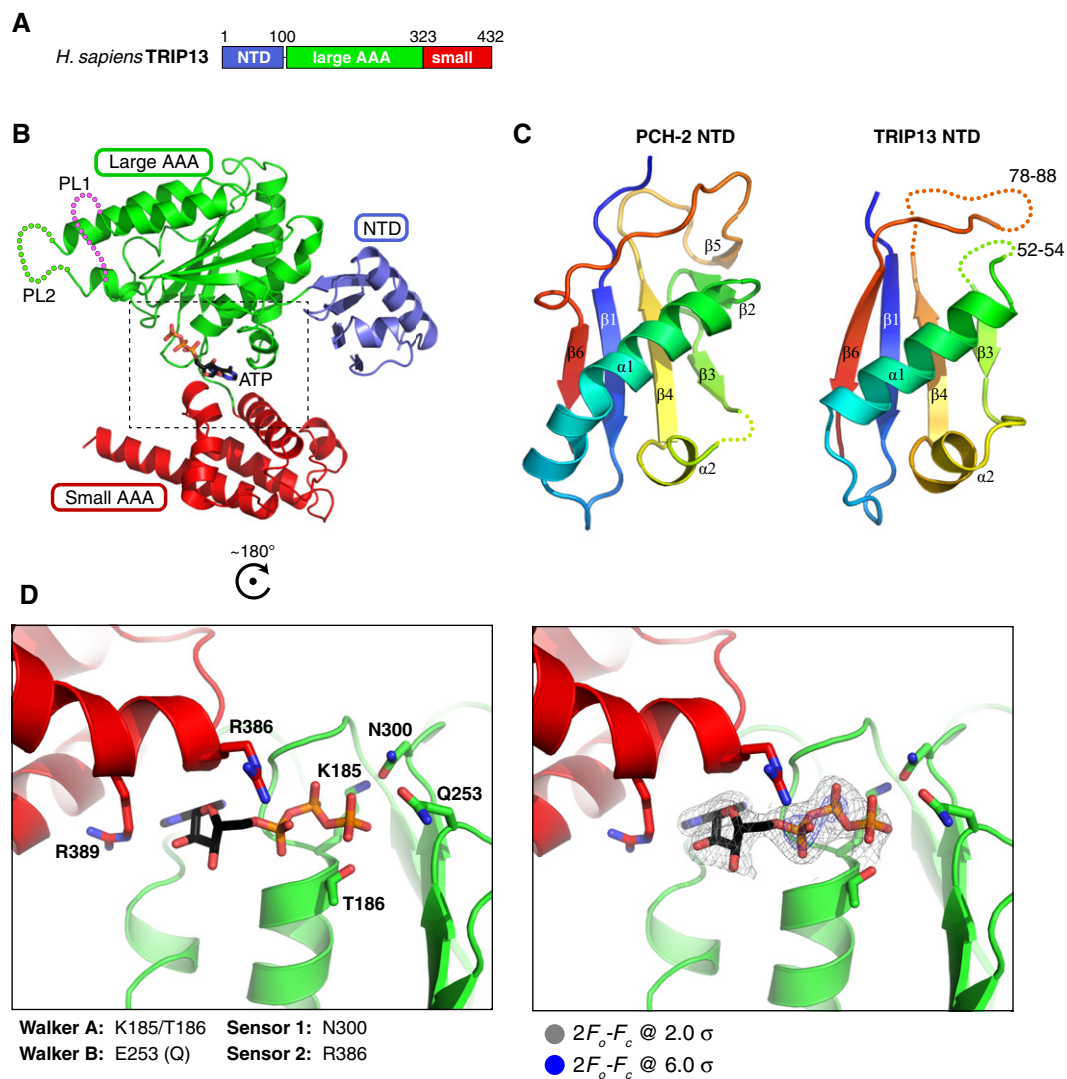
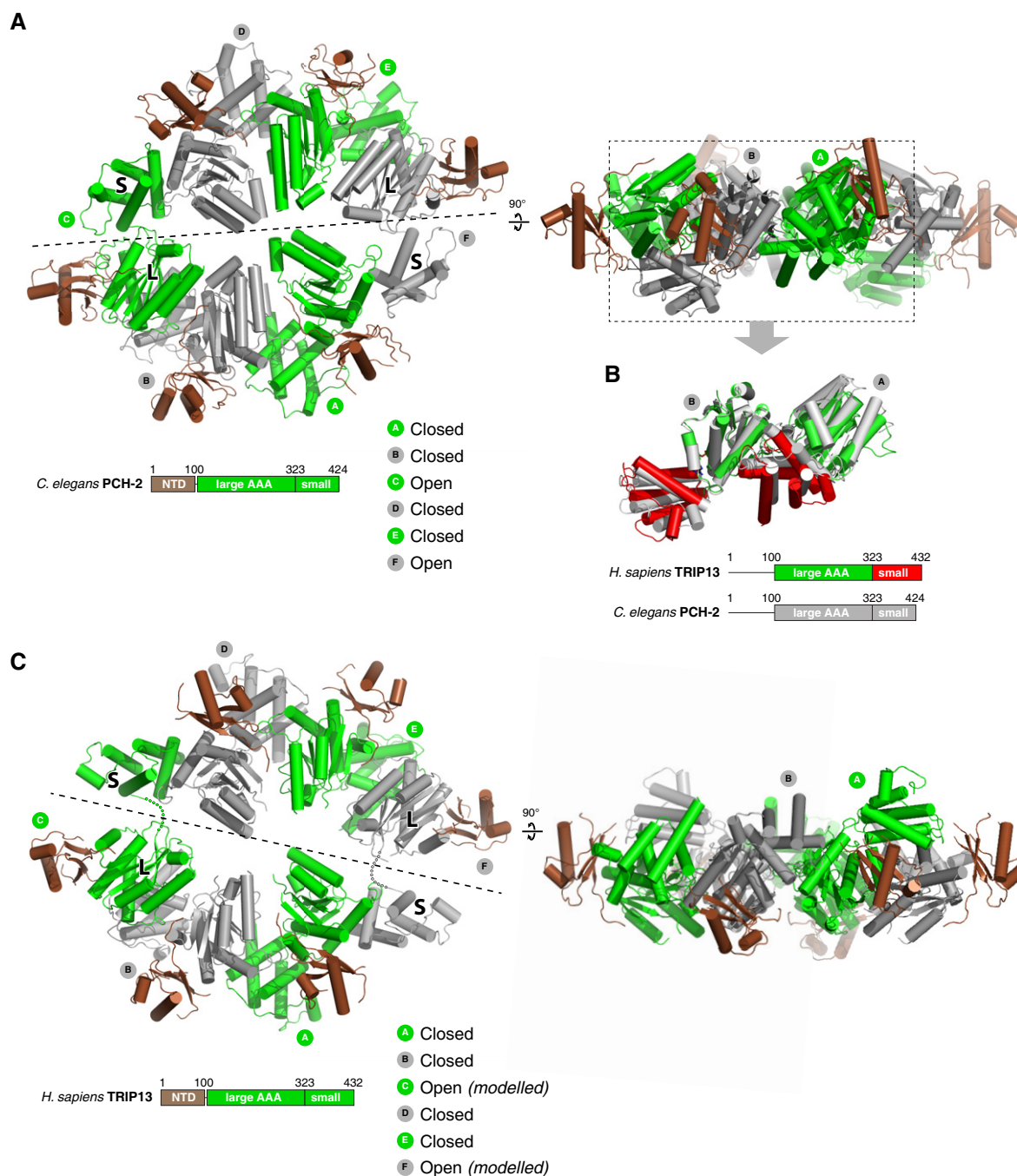


## Expanded View Figures



**Figure EV1. Structure and nucleotide binding of human TRIP13.**

- A Domain schematic of TRIP13, with N-terminal domain in blue and the large and small AAA ATPase subdomains in green and red, respectively.
- B Structure of a single TRIP13<sup>E253Q</sup> monomer, with domains colored as in panel (A). The two pore loops PL1 (pink; residues 217–226) and PL2 (green; residues 262–271) are disordered in the structure. PL1 contains W221, needed for coupling ATP hydrolysis to MAD2 engagement (Ye *et al.*, 2015) and lysines 220, 227, and 231, which crosslink to MAD2 in the ternary complex (Fig 2A).
- C Structural comparison of the PCH-2 (PDB ID 4XGU) (Ye *et al.*, 2015) and TRIP13 N-terminal domains (1.72 Å r.m.s.d. over 61 C $\alpha$  atom pairs). Disordered regions of TRIP13 (residues 52–54 and 78–88) are shown as dotted lines.
- D Close-up of ATP binding by TRIP13<sup>E253Q</sup>.



**Figure EV2. Modeling a closed TRIP13 hexamer.**

- A** Top and side views of the *Caenorhabditis elegans* PCH-2 hexamer (chains A/B from PDB ID 4XGU) (Ye *et al.*, 2015), with ATPase domains alternately colored gray and green, and NTDs in brown. Dashed line indicates the “half-hexamer” used as template for modeling a TRIP13 hexamer, splitting the “open” conformation C/F chains between the large and small AAA subdomains.
- B** Overlay of consecutive subunits in *C. elegans* PCH-2 (gray) and human TRIP13 (green/red). View is equivalent to the side view in panel (A), with NTDs removed for clarity. The large AAA subdomain of chain B was aligned between the two structures, with the location of chain A determined by non-crystallographic (PCH-2) or crystallographic (TRIP13) symmetry.
- C** Top and side views of a modeled TRIP13 hexamer. To model the TRIP13 hexamer, four consecutive subunits of the TRIP13 filament were aligned with either chains A, B or D, E of the *C. elegans* PCH-2 hexamer structure (Ye *et al.*, 2015) to generate “half-hexamer” models (split according to the dashed lines in the top views of panels A and C). For each half-hexamer, residues 1–320 of the first chain and 321–429 of the fourth chain, plus the entire second and third chains, were kept for the final “full-hexamer” model. The two resulting “open conformation” chains in the final model, in which residues 1–320 and 321–429 were modeled independently, show a ~17 Å distance between C $\alpha$  atoms of residues 320 and 321 (dotted lines).

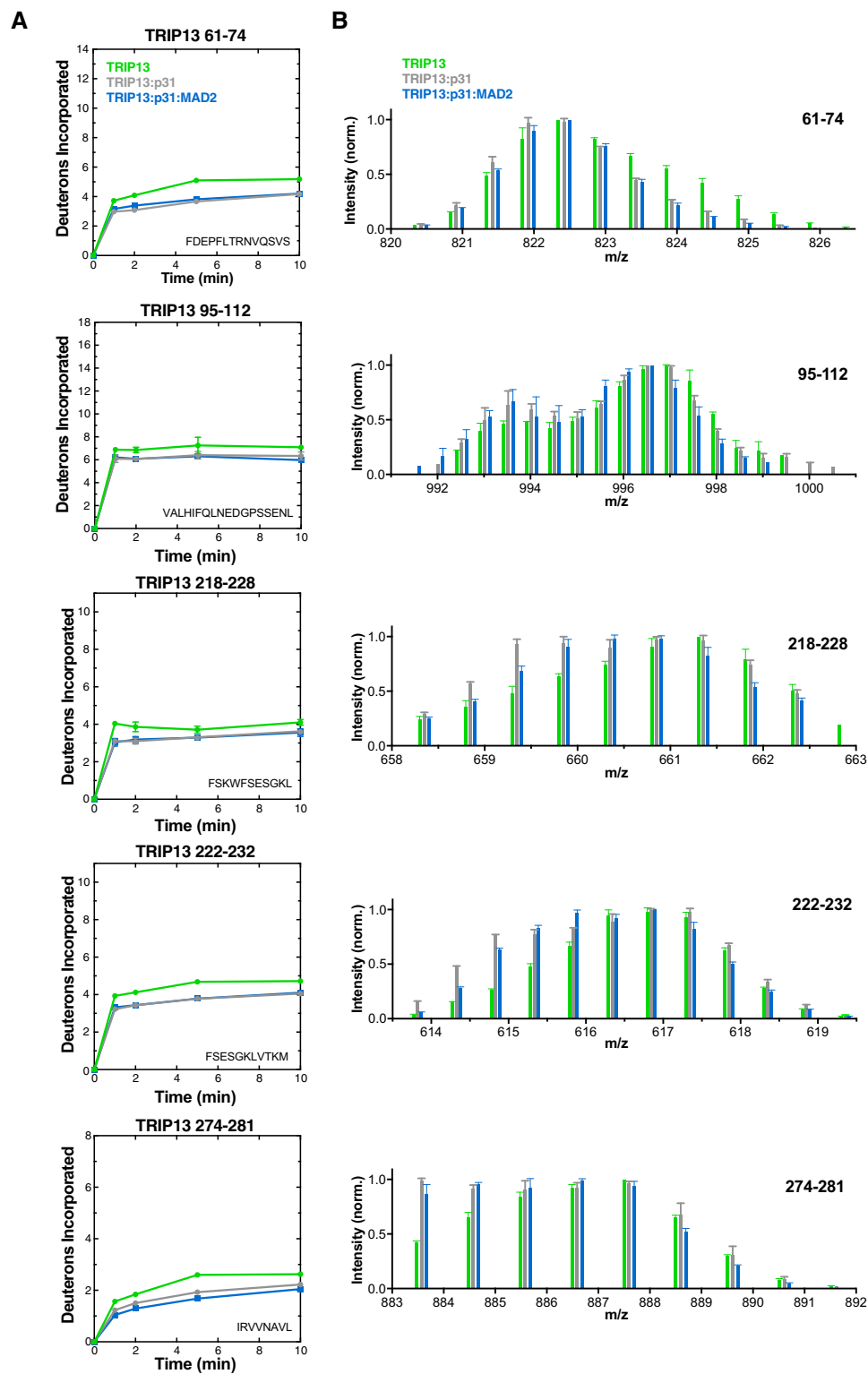


**Figure EV3. Bimodal peptides in TRIP13<sup>E253Q</sup> HDX-MS.**

A Deuterium uptake plots for TRIP13 peptides showing bimodality in HDX-MS analysis of one or more states (TRIP13<sup>E253Q</sup> alone green, TRIP13<sup>E253Q</sup>:p31<sup>comet</sup> gray, TRIP13<sup>E253Q</sup>:p31<sup>comet</sup>:MAD2 blue). Error bars represent standard deviation from triplicate measurements.

B Sticks (MS peak height versus mass/charge ratio, average and standard deviation of three independent samples) for TRIP13 peptides shown in panel (A). Each set of data shows peaks at the same m/z ratios; datasets are shifted on the graph for clarity.

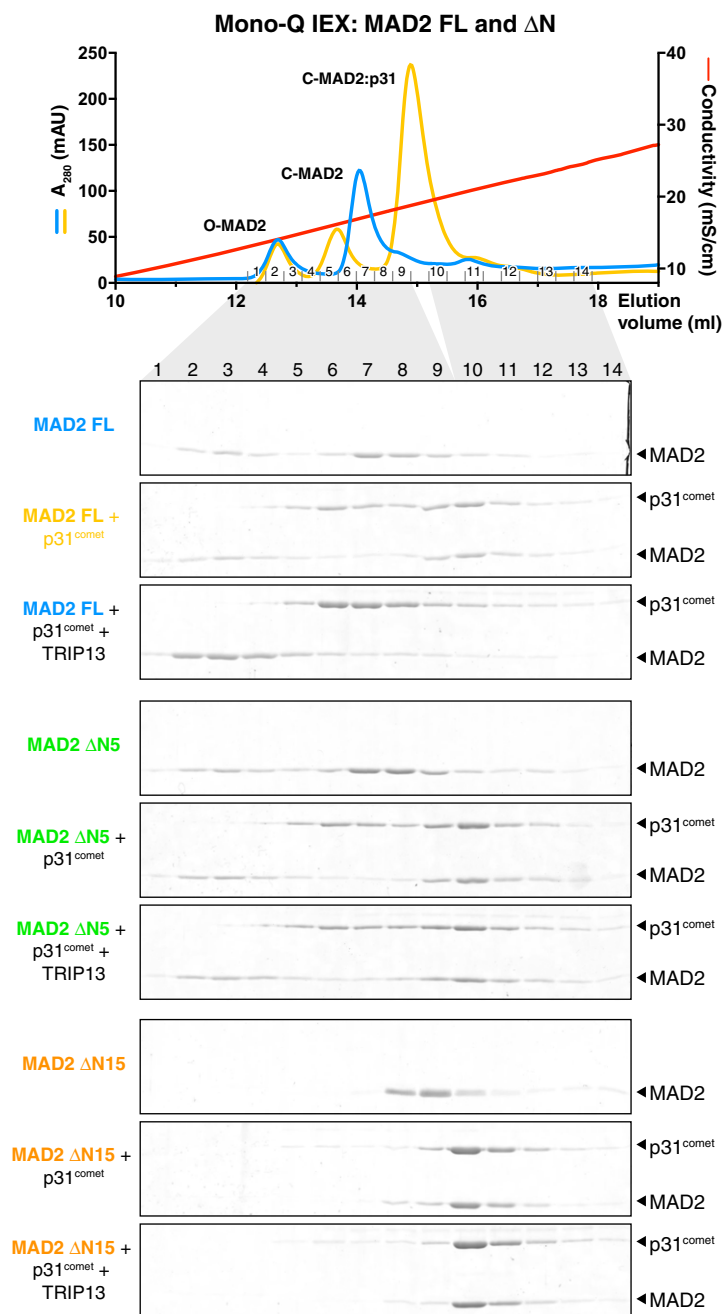


**Figure EV4. Ion-exchange separation of MAD2 conformers.**

Top: UV absorbance (280 nm) and conductivity traces, and associated fractions from Mono-Q ion-exchange separation of O- and C-MAD2. Samples shown are *Mus musculus* MAD2 FL (blue, same as Fig 4E, top panel) and MAD2 FL + p31<sup>comet</sup> (yellow, same as Fig 4E, second panel). Bottom: Mono-Q ion-exchange chromatography measuring conformational conversion of MAD2 FL (blue),  $\Delta$ N5 (green), and  $\Delta$ N15 (orange). Gels shown are the same as in Fig 4E, but are cropped to show both p31<sup>comet</sup> and MAD2.

